Weierstraß-Institut
für Angewandte Analysis und Stochastik

Leibniz-Institut im Forschungsverbund Berlin e. V.

Preprint ISSN 2198-5855

Variational modelling of porosity waves

Andrea Zafferi[1], Dirk Peschka[2]

submitted: August 11, 2025

[1] Freie Universität Berlin
Arnimallee 9
14195 Berlin
Germany
E-Mail: andrea.zafferi@fu-berlin.de

[2] Weierstrass Institute
Mohrenstr. 39
10117 Berlin
Germany
E-Mail: dirk.peschka@wias-berlin.de

No. 3210

Berlin 2025

2020 *Mathematics Subject Classification.* 74A15, 74F10, 74B20, 65M60.

Key words and phrases. Nonlinear poroelasticity, structure-preserving discretization, porosity waves.

DP thanks for the funding within the DFG Priority Program SPP 2171 Dynamic Wetting of Flexible, Adaptive, and Switchable Surfaces, project #422792530. AZ acknowledge the funding by the DFG-Collaborative Research Center 1114 Scaling Cascades in Complex Systems, project #235221301, C09 Dynamics of rock dehydration on multiple scales.

Edited by
Weierstraß-Institut für Angewandte Analysis und Stochastik (WIAS)
Leibniz-Institut im Forschungsverbund Berlin e. V.
Mohrenstraße 39
10117 Berlin
Germany

Fax: +49 30 20372-303
E-Mail: preprint@wias-berlin.de
World Wide Web: http://www.wias-berlin.de/

Variational modelling of porosity waves

Andrea Zafferi, Dirk Peschka

Abstract

Mathematical models for finite-strain poroelasticity in an Eulerian formulation are studied by constructing their energy-variational structure, which gives rise to a class of saddle-point problems. This problem is discretised using an incremental time-stepping scheme and a mixed finite element approach, resulting in a monolithic, structure-preserving discretisation. The Eulerian formulation is based on the inverse deformation, the so-called *reference map*. We present examples from geophysical applications, where elasticity and diffusive fluid flow are fully coupled and can be used to describe porosity waves, *i.e.*, localised ascending fluid waves driven by gravitational forces.

1 Introduction

Porosity waves play a critical role in various natural processes by governing fluid transport in deformable porous media. These waves typically emerge due to coupled pore pressure gradients, mechanical deformation of the porous matrix, and gravity. Depending on the context, these waves can be inertial, for example in ultrasound applications, or viscous, for example in geophysical processes on long timescales. Recent works have illustrated their importance across geophysical [1, 25, 24] and biological problems [7]. In particular [1] emphasizes on the interplay between compaction-driven fluid flow and plastic effects to generate localized fluid flow patterns, *i.e.*, solitary porosity waves. The classical works of Biot provided foundational theories of poroelasticity, describing wave propagation through fluid-saturated porous media [4, 5, 6], and were later extended by McKenzie [13]. However, accurately modelling porosity waves poses significant challenges, particularly due to the complexity inherent in coupling fluid-structure interactions and multiphase transport phenomena. Small-deformation models are often used but fail to capture the transition from small deformations of elastic solids to large deformations of soft solids or liquids.

A critical aspect of analysis and modelling poroelastic phenomena involves accurately capturing material deformation and fluid-solid interactions. Traditionally, Lagrangian approaches have been used for the mathematical treatment of these equations with large deformations, *e.g.*, [21, 26, 23]. In contrast, the use of the reference map technique has emerged as a valuable tool for handling finite-strain elasticity within Eulerian frameworks, successfully combining spatial and material viewpoints to enhance numerical robustness [11]. This approach has been effectively employed in modelling complex fluid-structure interactions [12] and extended to nonlinear elastic biological tissues, capturing their inherent compressibility and growth dynamics [27]. In a similar fashion, regarding geological applications an Eulerian large strain model for porous materials was developed in [22], where the energetics of the system is obtained as part of the mathematical analysis.

Modelling approaches that are based on thermodynamic principles rely on the definition of thermodynamic potentials such as energy or entropy and additional geometric structures or kinematic constructions involving conservation laws to deduce the evolution of the system. Within these frameworks, we highlight the Hamiltonian [15], damped Hamiltonian, and gradient system formulations [17], which naturally incorporate thermodynamic consistency and systematic treatment of dissipative processes. Among such approaches, one can find the GENERIC (General Equation for Non-Equilibrium Reversible-Irreversible Coupling) formalism, introduced by Grmela and Öttinger [9, 16], used to couple reversible and irreversible processes in isolated systems and later extended to thermoelastic solids and to damped Hamiltonian structure [14]. The development of corresponding structure-preserving discretisations promises to generate robust discrete schemes that also provide stable numerical methods for complex, nonlinearly coupled problems, *e.g.*, see [3, 10] in the context of GENERIC. Such

DOI 10.20347/WIAS.PREPRINT.3210 Berlin 2025

energy-based discretisation schemes have been also used in the context of poroelasticity, *e.g.*, in [8] or [2], where saddle-point problems are a reoccurring theme.

In this work, we build upon those structures and present a weak formulation of gradient systems, in the spirit of our previous work in [19] and in [28], for nonlinear poroelastic materials. The goal of this contribution is to highlight the origin of saddle-point structures and their natural discretisation for nonlinear poroelasticity using energy-based approaches. The paper is structured into two main parts. Section 2 deals with the thermodynamic modelling framework: from the abstract setting in 2.1, where we discuss an extension of classical gradient systems, to the application of this framework in 2.2 with the aim to derive a weak formulation of a partial differential equations system inspired by the phenomenon of porosity waves, and finally to the design of a structure preserving discretisation scheme in 2.3. In the last Section 3 we present the results of simulations for the above-mentioned model, focusing on two different regimes.

2 Variational modelling and discretisation

This section is dedicated to the introduction of an abstract modelling framework that relies on and extends the common notion of gradient systems. This approach offers a flexible way to model many interesting physical phenomena, as addressed in the introduction, while keeping the system thermodynamically consistent. This structured approach also lays the path towards the exploration of alternative formulations of physical systems, either in terms of different variables or in terms of a different set of coordinates. In this section we focus on a specific realization of this method concerning fluid flows of Stokes type. We conclude with the presentation of a discretisation for this model that naturally leads to the numerical implementations in the following Section 3.

2.1 Abstract variational setting

One way to describe a dissipative system, *i.e.*, a system where the total energy decreases over time due to friction, diffusion or other dissipative effects, is through an equation of the following form:

$$\mathbb{G}(\boldsymbol{q})\dot{\boldsymbol{q}} = -\mathbb{D}\mathscr{H}(\boldsymbol{q})\,, \quad \text{in } \mathcal{V}^*\,. \tag{1}$$

This equation can be characterized by three ingredients: the state space, *i.e.*, usually a subset of a Banach space, that we denote with $\mathcal{Q}$ with the associated elements being $\boldsymbol{q}$, the total or free energy of the system $\mathscr{H} : \mathcal{Q} \to \mathbb{R}$, and lastly the dissipation potential $\mathscr{R}(\boldsymbol{q}) : \mathcal{V} \to \mathbb{R}$ that acts on elements of the velocity space $\mathcal{V}$. Often, the velocity space can be identified with the state space itself, *i.e.*, $\mathcal{Q} \equiv \mathcal{V}$. Elements of the velocity space will be denoted by $\dot{\boldsymbol{q}}$ or $\partial_t \boldsymbol{q}$ when the velocity specific to the state variable $\boldsymbol{q}$ is taken or, more generally, by $\boldsymbol{v}$. We use $\langle\cdot,\cdot\rangle_{\mathcal{V}} : \mathcal{V}^* \times \mathcal{V} \to \mathbb{R}$ to indicate the canonical dual pairing $\langle\boldsymbol{\eta},\boldsymbol{v}\rangle_{\mathcal{V}} = \boldsymbol{\eta}(\boldsymbol{v})$ and we use $(\cdot,\cdot)_{\mathcal{V}} : \mathcal{V}\times\mathcal{V} \to \mathbb{R}$ for the L^2 inner product in $\mathcal{V} \subset L^2(\Omega)$. If the spaces are clear, then we drop the subscript. We use blackboard-bold symbols to denote operators on function spaces (except reals $\mathbb{R}$), and bold symbols to denote vectors, tensors, and other multicomponent objects (except coordinates $x \in \Omega \subset \mathbb{R}^d$).Variations of the energy $\mathscr{H}$ will be computed through the *Frechét* derivative $\mathbb{D}\mathscr{H}(\boldsymbol{q}) \in \mathcal{V}^*$:

$$\langle\mathbb{D}\mathscr{H}(\boldsymbol{q}),\boldsymbol{v}\rangle_{\mathcal{V}} := \lim_{h\to 0} \frac{\mathscr{H}(\boldsymbol{q}+h\boldsymbol{v}) - \mathscr{H}(\boldsymbol{q})}{h}\,, \text{ for any } \boldsymbol{v} \in \mathcal{V}\,. \tag{2}$$

Throughout this paper we will assume $\mathscr{R}(\boldsymbol{q},\cdot)$ to be convex and quadratic for any $\boldsymbol{v} \in \mathcal{V}$, *i.e.*,

$$\mathscr{R}(\boldsymbol{q},\boldsymbol{v}) = \frac{1}{2}\langle\mathbb{G}(\boldsymbol{q})\boldsymbol{v},\boldsymbol{v}\rangle_{\mathcal{V}}\,, \tag{3}$$

where $\mathbb{G}(\boldsymbol{q}) : \mathcal{V} \to \mathcal{V}^*$ is the associated positive symmetric operator. Hence, in order to represent this evolution equation we can simply write the triple $(\mathcal{Q},\mathscr{H},\mathbb{G})$, known as classical gradient system, or $(\mathcal{Q},\mathscr{H},\mathscr{R})$ for more general ones. An alternative formulation relies on the application of the *Legendre transform*, through which we

can define the dual dissipation potential for any element $\boldsymbol{\eta} \in \mathcal{V}^*$ by $\mathscr{R}^*(\boldsymbol{q}, \boldsymbol{\eta}) := \sup_{\boldsymbol{v}\in\mathcal{V}} \left(\langle \boldsymbol{\eta}, \boldsymbol{v}\rangle_{\mathcal{V}} - \mathscr{R}(\boldsymbol{q}, \boldsymbol{v})\right)$. By applying the definition of $\mathscr{R}^*$ we introduce the Onsager operator $\mathbb{K}(\boldsymbol{q}) : \mathcal{V}^* \to \mathcal{V}$ from the relation $\mathscr{R}^*(\boldsymbol{q}, \boldsymbol{\eta}) = \frac{1}{2}\left\langle \boldsymbol{\eta}, \mathbb{G}(\boldsymbol{q})^{-1}\boldsymbol{\eta}\right\rangle = \frac{1}{2}\langle \boldsymbol{\eta}, \mathbb{K}(\boldsymbol{q})\boldsymbol{\eta}\rangle$. Together with (1), this results in an alternative evolution equation taking place on the velocity space

$$\dot{\boldsymbol{q}} = -\mathbb{K}(\boldsymbol{q})\mathbb{D}\mathscr{H}(\boldsymbol{q})\,, \quad \text{in } \mathcal{V}\,. \tag{4}$$

Both equations (1) and (4) appear in strong form. One way to extend (4) to a saddle-point problem and to a weak formulation is to consider the auxiliary space $\mathcal{W}$ and a linear transformation $\mathbb{M}^*(\boldsymbol{q}) : \mathcal{W} \to \mathcal{V}^*$ that provides a representation of the generalized forces $\boldsymbol{\eta} \in \mathcal{V}^*$ and thus of the driving force $\mathbb{M}^*(\boldsymbol{q})\boldsymbol{w} = \mathbb{D}\mathscr{H}(\boldsymbol{q})$. Based on its definition and the adjoint operator $\mathbb{M}(\boldsymbol{q}) : \mathcal{V} \to \mathcal{W}^*$, *i.e.*, $\langle \mathbb{M}^*(\boldsymbol{q})\boldsymbol{w}, \boldsymbol{v}\rangle_{\mathcal{V}} = \langle \mathbb{M}(\boldsymbol{q})\boldsymbol{v}, \boldsymbol{w}\rangle_{\mathcal{W}}$, one can rewrite equation (4) as a weak form of a saddle-point problem

$$\begin{aligned} k(\boldsymbol{q}; \boldsymbol{\eta}, \boldsymbol{w}) + b(\boldsymbol{q}; \dot{\boldsymbol{q}}, \boldsymbol{w}) &= 0 && \text{for all } \boldsymbol{w} \in \mathcal{W}\,, && \text{(5a)}\\ b(\boldsymbol{q}; \boldsymbol{v}, \boldsymbol{\eta}) &= \langle \mathbb{D}\mathscr{H}(\boldsymbol{q}), \boldsymbol{v}\rangle_{\mathcal{V}} && \text{for all } \boldsymbol{v} \in \mathcal{V}\,, && \text{(5b)} \end{aligned}$$

where $k(\boldsymbol{q}; \boldsymbol{\eta}, \boldsymbol{w}) = \langle \mathbb{M}^*(\boldsymbol{q})\boldsymbol{w}, \mathbb{K}(\boldsymbol{q})\mathbb{M}^*(\boldsymbol{q})\boldsymbol{\eta}\rangle_{\mathcal{V}}$ arises from the dual dissipation potential and therefore is symmetric, positive definite and $b(\boldsymbol{v}, \boldsymbol{w}) = \langle \mathbb{M}(\boldsymbol{q})^*\boldsymbol{w}, \boldsymbol{v}\rangle_{\mathcal{V}}$.

This weak formulation actually permits us to go one step further and include additional dissipative effects acting on the velocities $\boldsymbol{v} \in \mathcal{V}$, instead of the generalized forces $\mathbb{M}^*(\boldsymbol{q})\boldsymbol{\eta}$, by introducing a symmetric, positive operator $\mathbb{G}(\boldsymbol{q}) : \mathcal{V} \to \mathcal{V}^*$ associated to the bilinear form $g(\boldsymbol{q}; \boldsymbol{v}_1, \boldsymbol{v}_2) = \langle \mathbb{G}(\boldsymbol{q})\boldsymbol{v}_1, \boldsymbol{v}_2\rangle_{\mathcal{V}} = \langle \mathbb{D}_{v_1}\mathscr{R}(\boldsymbol{q}, \boldsymbol{v}_1), \boldsymbol{v}_2\rangle_{\mathcal{V}}$. System (5) then becomes:

$$\begin{aligned} k(\boldsymbol{q}; \boldsymbol{\eta}, \boldsymbol{w}) + b(\boldsymbol{q}; \dot{\boldsymbol{q}}, \boldsymbol{w}) &= 0 && \text{for all } \boldsymbol{w} \in \mathcal{W}\,, && \text{(6a)}\\ b(\boldsymbol{q}; \boldsymbol{v}, \boldsymbol{\eta}) - g(\boldsymbol{q}; \dot{\boldsymbol{q}}, \boldsymbol{v}) &= \langle \mathbb{D}\mathscr{H}(\boldsymbol{q}), \boldsymbol{v}\rangle_{\mathcal{V}} && \text{for all } \boldsymbol{v} \in \mathcal{V}\,. && \text{(6b)} \end{aligned}$$

Observe that in the case $k(\boldsymbol{q}; \cdot, \cdot) \equiv 0$, the equations (6) reduce simply to a weak formulation of (1). The dissipative nature of the system is preserved under this construction and it can be verified by testing as usual with velocity $\boldsymbol{v} = \dot{\boldsymbol{q}}$ and chemical potential $\boldsymbol{w} = \boldsymbol{\eta}$ and by subtracting the equations (6)

$$\frac{\mathrm{d}}{\mathrm{d}t}\mathscr{H}\big(\boldsymbol{q}(t)\big) = \langle \mathbb{D}\mathscr{H}(\boldsymbol{q}), \dot{\boldsymbol{q}}\rangle_{\mathcal{V}} = -\Big(k(\boldsymbol{q}; \boldsymbol{\eta}, \boldsymbol{\eta}) + g(\boldsymbol{q}; \dot{\boldsymbol{q}}, \dot{\boldsymbol{q}})\Big) \leq 0\,.$$

2.2 Eulerian poroelastic model

Kinematics. To instantiate this abstract framework, we develop an Eulerian model tailored to poroelastic media. Consider a state vector composed of an Eulerian vector field (displacement) and a conserved scalar field (concentration)

$$\boldsymbol{q} = \begin{pmatrix} \boldsymbol{u} : \Omega \to \mathbb{R}^d \\ c : \Omega \to \mathbb{R} \end{pmatrix} \in \mathcal{Q}\,, \tag{8}$$

where the displacement $\boldsymbol{u}$ is computed using the composition of the Lagrangian displacement and the reference map, *i.e.*, $\boldsymbol{u}(t, x) := x - \boldsymbol{\alpha}(t, x), x = (x_1, \ldots, x_d)^\top$ and c represents the particle concentration. Before we continue with the formulation, we shortly recall the notion of Lagrangian and Eulerian representation. Consider a domain $\Omega_t \subset \mathbb{R}^d$ where the system is evolving at time $t > 0$. This is usually regarded as the Eulerian or actual configuration of the system. The Lagrangian or reference representation relies on the existence assumption of an *original* state or a past configuration of the system Ω_0 that for convenience is set at time $t = 0$. These two configurations can be linked through a map that we call *flow map* that relates points or particles from the reference configuration to the current configuration, *i.e.*, $x = \boldsymbol{\chi}(t, \bar{x})$ where $x \in \Omega_t$ and $\bar{x} \in \Omega_0$. This relation can always be constructed if, *e.g.*, given a regular enough velocity field $\boldsymbol{v}$ one solves the Cauchy problem

$$\begin{aligned} \frac{\partial \boldsymbol{\chi}(t, \bar{x})}{\partial t} &= \boldsymbol{v}(t, \boldsymbol{\chi}(t, \bar{x}))\,, && \text{for all } t > 0, \bar{x} \in \Omega_0\,, && \text{(9)}\\ \boldsymbol{\chi}(0, \bar{x}) &= \bar{x}\,, && \text{for all } \bar{x} \in \Omega_0\,. && \text{(10)} \end{aligned}$$

The inverse of the flow map, *i.e.*, the mapping reconstructing the inverse motion of a particle, will be denoted by $\boldsymbol{\alpha}$. Figure 1 exemplarily shows the Lagrangian and Eulerian configuration with the related maps.

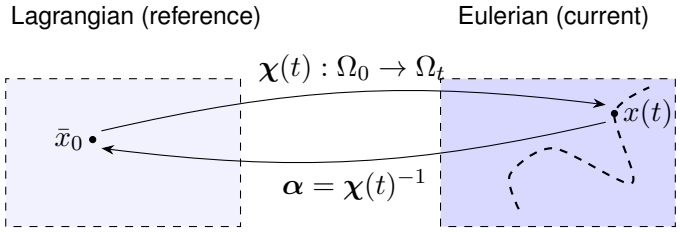

Figure 1: Flow map $\boldsymbol{\chi}$ from Lagrangian to Eulerian configuration and its reference map $\boldsymbol{\alpha} = \boldsymbol{\chi}^{-1}$. The dashed curve shows a possible particle trajectory so that $x(t) = \boldsymbol{\chi}(t, \bar{x}_0)$.

The Lagrangian configuration is particularly useful for the description of solids, where strains and stresses appear in a simplified form, while for fluids, where strong topological changes usually occurs, an Eulerian formulation is more favourable to avoid mesh distortion. With this in mind, a commonly employed *Lagrangian* variable is the displacement $\bar{\boldsymbol{u}}(t, \bar{x}) := \boldsymbol{\chi}(t, \bar{x}) - \bar{x}$, whose corresponding *Eulerian* variable is $\boldsymbol{u}$ in (8). We will consider a domain whose boundary stays fixed over time, therefore we will drop the subscript and write $\Omega \equiv \Omega_t$. We conclude this paragraph with fundamental relations between the Eulerian displacement $\boldsymbol{u}$:

$$\partial_t \boldsymbol{u}(t,x) = -\partial_t \boldsymbol{\alpha}(t,x)\,, \tag{11a}$$
$$\partial_t \boldsymbol{\alpha}(t,x) = -(\nabla \boldsymbol{\alpha})\boldsymbol{v}(t,x)\,, \tag{11b}$$
$$\boldsymbol{F}(t,x) := (\nabla \boldsymbol{\alpha})^{-1}(t,x)\,, \qquad \textit{Eulerian deformation gradient} \tag{11c}$$

where $\boldsymbol{v}$ denotes the Eulerian velocity field. By combining (11a) and (11b) and (11c) we get

$$\boldsymbol{F}(t,x)\partial_t \boldsymbol{u}(t,x) = \boldsymbol{v}(t,x)\,, \tag{11d}$$

where the Eulerian deformation gradient $\boldsymbol{F}$ can also be represented as

$$\boldsymbol{F}(t,x) = (\nabla \boldsymbol{\alpha})^{-1}(t,x) = (\boldsymbol{I}_d - \nabla \boldsymbol{u}(t,x))^{-1}\,, \tag{11e}$$

Differentiating the identity $\boldsymbol{u}(t, \boldsymbol{\chi}(t, \bar{\boldsymbol{x}})) = \bar{\boldsymbol{u}}(t, \bar{\boldsymbol{x}})$ with respect to time we get the relation

$$\partial_t \boldsymbol{u} = (\boldsymbol{I}_d - \nabla \boldsymbol{u})\, \partial_t \bar{\boldsymbol{u}}\,. \tag{11f}$$

Given the Jacobian $J := \det \boldsymbol{F}$ we state some chain rules helpful in the computation of gradients and determinant of $\boldsymbol{F}$ and J, cf. [20, eq.(62)],

$$\mathbb{D}_{\boldsymbol{u}} J = J\boldsymbol{F}^{\top} : \nabla \square\,, \tag{11g}$$
$$\mathbb{D}_{\boldsymbol{u}} f(\boldsymbol{F}) = \boldsymbol{F}^{\top}\left(\partial_{\boldsymbol{F}} f(\boldsymbol{F})\right)\boldsymbol{F}^{\top} : \nabla \square\,. \tag{11h}$$

Energetics and weak form. The second necessary ingredient for the formulation of our system is the total energy $\mathscr{H}$. We consider an energy functional $\mathscr{H} : \mathcal{Q} \to \mathbb{R}$ with $\boldsymbol{q} = (\boldsymbol{u}, c)$ that is expressed in the following form:

$$\mathscr{H}(\boldsymbol{q}) := \int_\Omega H_{\mathrm{el}}(\boldsymbol{F}) + H_{\mathrm{Biot}}(J,c) + H_{\mathrm{grav}}(c) + \frac{\varepsilon}{2}|\nabla c|^2 \,\mathrm{d}x\,, \tag{12a}$$
$$H_{\mathrm{el}}(\boldsymbol{F}) := \tfrac{\mu}{2}\mathrm{tr}(\boldsymbol{C} - \boldsymbol{I}_d)\,, \qquad \text{with } \boldsymbol{C} = (\boldsymbol{F}^{\top}\boldsymbol{F})/J^{2/d}\,, \tag{12b}$$
$$H_{\mathrm{Biot}}(J,c) := \tfrac{1}{2}\pi^2\,, \qquad \text{with } \pi = (c - c^*) - (J-1)\,, \tag{12c}$$
$$H_{\mathrm{grav}}(c) := c g_0 x_d\,, \tag{12d}$$

The functional is composed by four terms: H_{el} captures the elastic behaviour of the material only through the isochoric part of the right Cauchy-Green deformation tensor, H_{Biot} couples displacement and concentration relating volumetric changes in the volume J with concentration variations from the steady state c^* with a Biot-like pressure π, H_{grav} collects the external forces, which in our case amount to gravity alone and are parallel to the direction of the last dth coordinate and finally a higher order regularizing term for c. We write the weak formulation in terms of functions $\boldsymbol{v} = (\boldsymbol{v_u}, v_c) \in \mathcal{V}$ and with the auxiliary space $w = w_c \in \mathcal{W}$. The total energy (12) generates the following driving force, cf. (2):

$$\begin{aligned}\langle \mathbb{D}\mathscr{H}(\boldsymbol{q}), \boldsymbol{v}\rangle &= \int_\Omega \boldsymbol{F}^\top \partial_{\boldsymbol{F}} \left(H_{\mathrm{el}}\right) \boldsymbol{F}^\top : \nabla \boldsymbol{v_u} - \pi J \boldsymbol{F}^\top : \nabla \boldsymbol{v_u} + \pi v_c + g_0 x_d v_c + \varepsilon \nabla c \cdot \nabla v_c \\ &= \int_\Omega \left(\tfrac{\mu}{2}\left(2\boldsymbol{C} - \tfrac{2}{d}\mathrm{tr}(\boldsymbol{C})\boldsymbol{I}_d\right) - \pi J\right) \boldsymbol{F}^\top : \nabla \boldsymbol{v_u} + (\pi + g_0 x_d) v_c + \varepsilon \nabla c \cdot \nabla v_c\end{aligned} \tag{13}$$

The representation of elements of the dual space $\mathcal{V}^*$ is given through the bilinear for b and the map $\mathbb{M} : \mathcal{V} \to \mathcal{W}^*$:

$$\langle \mathbb{M}\boldsymbol{v}, w_c\rangle_{\mathcal{W}} = b(\boldsymbol{q}; \boldsymbol{v}, w_c) := \int_\Omega w_c \left(v_c - \nabla \cdot (c\boldsymbol{F}\boldsymbol{v_u})\right) \,\mathrm{d}x\,. \tag{14}$$

One might already notice the presence of advective terms in (14), however this is not the solely way in our variational framework to include such contributions, *e.g.*, these terms can be derived from a damped Hamiltonian system alike (5). This was the strategy employed to study fluid-structure interaction problems in [19]. There this contribution naturally arose from a weak formulation that included the operator for thermodynamically reversible processes, sometimes called *Poisson operator* or *Poisson brackets*. This operator has a fairly simple expression in Lagrangian coordinates and in order to recover the Eulerian formulation we apply a transformation mechanism based on the flow map defined in (9) that preserves the bilinear forms present in (5). With this identification we are ready to compute the remaining two dissipative bilinear forms

$$\langle \mathbb{M}^* w_1, \mathbb{K}(\boldsymbol{q})\mathbb{M}^* w_2\rangle_{\mathcal{V}} = k(\boldsymbol{q}; w_1, w_2) := \int_\Omega \nabla w_1 \cdot D(c) \nabla w_2 \mathrm{d}x \qquad \text{with } D(c) = \tfrac{D_0}{2} c^2\,, \tag{15}$$

$$\langle \mathbb{G}(\boldsymbol{q})\boldsymbol{v}_1, \boldsymbol{v}_2\rangle_{\mathcal{V}} = g(\boldsymbol{q}; \boldsymbol{v}_{1,\boldsymbol{u}}, \boldsymbol{v}_{2,\boldsymbol{u}}) := \int_\Omega \nu \nabla_{\mathrm{s}}(\boldsymbol{F}\boldsymbol{v}_{1,\boldsymbol{u}}) : \nabla_{\mathrm{s}}(\boldsymbol{F}\boldsymbol{v}_{2,\boldsymbol{u}}) \,\mathrm{d}x \quad \text{with } \nabla_{\mathrm{s}}\boldsymbol{a} = \tfrac{1}{2}\nabla \boldsymbol{a} + \tfrac{1}{2}(\nabla \boldsymbol{a})^\top\,, \tag{16}$$

where $\boldsymbol{v}_1, \boldsymbol{v}_2 \in \mathcal{V}, w_1, w_2 \in \mathcal{W}$. Altogether the system formally reads:

$$k(\boldsymbol{q}; \xi_c, \eta_c) + (\xi_c, \dot{c}) + (\xi_c, \mathrm{div}(c\boldsymbol{F}\dot{\boldsymbol{u}})) = 0\,, \tag{17a}$$

$$-g(\boldsymbol{q}; \dot{\boldsymbol{u}}, \boldsymbol{v_u}) + (\eta_c, \mathrm{div}(c\boldsymbol{F}\dot{\boldsymbol{v}}_{\boldsymbol{u}})) + (\eta_c, v_c) = \langle \mathbb{D}\mathscr{H}(\boldsymbol{q}), \boldsymbol{v}\rangle\,. \tag{17b}$$

Thus we obtain the following weak system of equations for any $(\boldsymbol{v_u}, v_c) \in \mathcal{V}$ and $\xi_c \in \mathcal{W}$:

$$(\nu \nabla_{\mathrm{s}}(\boldsymbol{F}\dot{\boldsymbol{u}}), \nabla_{\mathrm{s}}(\boldsymbol{F}\boldsymbol{v_u})) + (\eta_c, \mathrm{div}(c\boldsymbol{F}\boldsymbol{v_u})) = \left(\boldsymbol{F}^\top \partial_{\boldsymbol{F}}\left(H_{\mathrm{el}}\right)\boldsymbol{F}^\top, \nabla \boldsymbol{v_u}\right) - \left(\pi J \boldsymbol{F}^\top, \nabla \boldsymbol{v_u}\right) \tag{18a}$$

$$(\xi_c, \dot{c}) + (\xi_c, \mathrm{div}(c\boldsymbol{F}\dot{\boldsymbol{u}})) = (\nabla \xi_c, D(c)\nabla \eta_c)\,, \tag{18b}$$

$$(\eta_c, v_c) = (\pi + g_0 x_d, v_c) + (\varepsilon \nabla c, \nabla v_c)\,. \tag{18c}$$

The system is complemented with no-slip on the sides and homogeneous Dirichlet on the top and the bottom boundary conditions for $\boldsymbol{u}$, *i.e.*, $\boldsymbol{u} \cdot \boldsymbol{\nu} = 0$, where $\boldsymbol{\nu}$ is the normal outer vector, and $\boldsymbol{u} = 0$, and with homogenous Neumann boundary conditions for c, *i.e.*, $D(c)\nabla \eta_c \cdot \boldsymbol{\nu} = 0$.

2.3 Discretization

Below we describe a structure-preserving discretisation of the poroelastic model. To this end, we are going to discretise (6) using finite elements in space and using a semi-implicit scheme in time. Therefore, the derivative

of the energy is discretise fully implicitly and the state-dependence of the bilinear forms in (6) are discretised explicitly in $\boldsymbol{q}$ are implicitly in all remaining variables. Therefore, for a given triangulation $\mathcal{T}_h$ of the domain $\Omega = \bigcup_{T\in\mathcal{T}_h} T$ introduce the auxiliary finite-dimensional function space

$$V_h^{m,k} = \left\{ v \in C^1(\Omega;\mathbb{R}^m) \,:\, v_i|_e \in P_k(T),\, T\in\mathcal{T}_h,\, i\in\{1,...,m\} \right\} \tag{19}$$

where $m = 1$ for scalar functions and $m = d$ for vector fields and k is the polynomial degree of the H^1 conforming function on elements $T \in \mathcal{T}_h$. For the discretisation we write $\boldsymbol{q}^k = \boldsymbol{q}(t^k)$ and $\boldsymbol{\eta}^k = \boldsymbol{\eta}(t^k)$ for times $t^0 = 0 < t^1 < \ldots < t^N = T$ and discretise

$$\boldsymbol{q}^k = (\boldsymbol{u}^k, \boldsymbol{c}^k) = V_h^{d,2} \times V_h^{1,1} =: \mathcal{V}_h \qquad \text{and} \qquad \boldsymbol{\eta}^k = V_h^{1,1} =: \mathcal{W}_h\,, \tag{20}$$

where the space for $\boldsymbol{u}^k$ is complemented with suitable Dirichlet boundary conditions $\boldsymbol{u}^k\cdot\boldsymbol{\nu} = 0$ (sliding) or $\boldsymbol{u}^k = 0$ (no-slip) to be specified later on parts of $\partial\Omega$. For a given $\boldsymbol{q}^{k-1}$, we seek $\boldsymbol{q}^k$ and $\boldsymbol{\eta}^k$ such that

$$k(\boldsymbol{q}^{k-1};\boldsymbol{\eta}^k,\boldsymbol{w}) + b(\boldsymbol{q}^{k-1};\tfrac{\boldsymbol{q}^k-\boldsymbol{q}^{k-1}}{\tau^k},\boldsymbol{w}) \qquad = 0 \qquad \text{for all } \boldsymbol{w}\in\mathcal{W}_h\,, \tag{21a}$$

$$b(\boldsymbol{q}^{k-1};\boldsymbol{v},\boldsymbol{\eta}^k) - g(\boldsymbol{q}^{k-1};\tfrac{\boldsymbol{q}^k-\boldsymbol{q}^{k-1}}{\tau^k},\boldsymbol{v}) \qquad = \left\langle \mathbb{D}\mathscr{H}(\boldsymbol{q}^k),\boldsymbol{v}\right\rangle_{\mathcal{V}} \qquad \text{for all } \boldsymbol{v}\in\mathcal{V}_h\,. \tag{21b}$$

where $\tau^k = t^k - t^{k-1}$. In [23] we showed that such discretisation scheme corresponds to an incremental minimization scheme for $\boldsymbol{q}^k$. The form above in (21) produces a (nonlinear) saddle-point problem, which is solved using a Newton method. We solve this problem with a constant time step size $\tau^k \equiv \tau$ for all $k \in \{1,...,N\}$. Equation (21) is a semi-implicit *monolithic structure-preserving discretisation* of the gradient flow equation (4) or the corresponding saddle-point structure (6).

3 Porosity wave example: flow vs diffusion

The strong form of the system (18) gives rise to the poroelastic model

$$-\nu\,\mathrm{div}\nabla_{\mathrm{s}}(\boldsymbol{F}\dot{\boldsymbol{u}}) + c\nabla\eta_c = \mathrm{div}(\boldsymbol{\sigma}) \quad \text{where} \quad \boldsymbol{\sigma} = \partial_{\boldsymbol{F}} H_{\mathrm{el}}\boldsymbol{F}^\top + H_{\mathrm{el}}\boldsymbol{I}_d + (\tfrac{1}{2}\pi^2 - J\pi)\boldsymbol{I}_d\,, \tag{22a}$$

$$\dot{c} + \mathrm{div}(c\boldsymbol{F}\dot{\boldsymbol{u}}) = -\,\mathrm{div}\left(D(c)\nabla\eta_c\right)\,, \tag{22b}$$

where $\pi = (c-c^*) - (J-1)$ and $\eta_c = \pi + g_0 x_d - \varepsilon\Delta c$ and isochoric right Cauchy-Green deformation tensor $\mathbb{C} = \boldsymbol{F}^\top\boldsymbol{F}/(\det\boldsymbol{F})^{2/d}$. This is an Eulerian model for large deformations and models the viscous relaxation of the compressible elastic body by shear forces and Biot-type pore pressure encoded in the Cauchy stress $\boldsymbol{\sigma}$. Using (11d) we can introduce the Eulerian solid velocity $\boldsymbol{v} = \boldsymbol{F}\dot{\boldsymbol{u}}$.

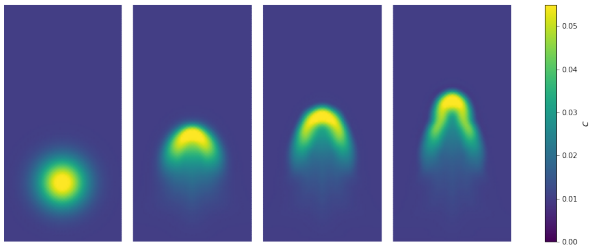

(a) Concentration c for time advancing from left to right.

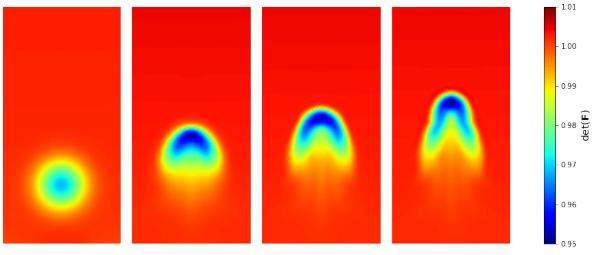

(b) Determinant $J = \det\boldsymbol{F}$ for time advancing from left to right.

Figure 2: Porosity wave moving fluid upwards and displacing the (elastic) material in the **flowing regime** at times $t = 0, 10/3, 20/3, 10$.

Remark 1. Note that by defining the elastic Lagrangian energy as $\bar{H}_{\mathrm{el}} = H_{\mathrm{el}}J$ one recovers the classical elastic Cauchy stress in (22a) for the elastic contribution and in a similar manner one can define the reference $\bar{H}_{\mathrm{Biot}}$ and recover the common expression for the thermodynamic pressure. The main step in the derivation of the elastic Cauchy stress tensor, where for the sake of simplicity we write $H = H_{\mathrm{el}}$, is the following computation:

$$\begin{aligned}\boldsymbol{F}^{-\top}\mathrm{div}\left(\boldsymbol{F}^{\top}\frac{\partial H}{\partial \boldsymbol{F}}\boldsymbol{F}^{\top}\right) &= \boldsymbol{F}^{-\top}_{ij}\nabla_k\left(\boldsymbol{F}^{\top}_{jl}\frac{\partial H}{\partial \boldsymbol{F}_{lm}}\boldsymbol{F}^{\top}_{mk}\right)\\ &= \boldsymbol{F}^{-\top}_{ij}\boldsymbol{F}^{\top}_{jl}\nabla_k\left(\frac{\partial H}{\partial \boldsymbol{F}_{lm}}\boldsymbol{F}^{\top}_{mk}\right) + \boldsymbol{F}^{-1}_{ji}\frac{\partial H}{\partial \boldsymbol{F}_{lm}}\boldsymbol{F}_{km}\bar{\nabla}_j(\boldsymbol{F}_{ln})\boldsymbol{F}^{-1}_{nk}\\ &= \mathrm{div}\left(\partial_{\boldsymbol{F}}H\boldsymbol{F}^{\top}\right) + \frac{\partial H}{\partial \boldsymbol{F}_{lm}}\bar{\nabla}_j(\boldsymbol{F}_{lm})\boldsymbol{F}^{-1}_{ji} = \mathrm{div}\left(\partial_{\boldsymbol{F}}H\boldsymbol{F}^{\top} + H\boldsymbol{I}_d\right),\end{aligned}$$

where the sum over the same indices has to be taken, we have made use of the identity relating Eulerian spatial derivatives with the third order deformation tensor $\nabla_k\boldsymbol{F}_{lj} = \bar{\nabla}_s\boldsymbol{F}_{lj}\boldsymbol{F}^{-1}_{sk}$, $\bar{\nabla}_s\boldsymbol{F}_{lj} = \bar{\nabla}^2_{sj}\boldsymbol{\chi}_l$ with $\boldsymbol{\chi}$ being the flowmap, and in the last equality we applied the chain rule for ∇H.

There are a couple of peculiarities of this model that we want to briefly comment on. Firstly, the diffusive model is of fourth order due to the regularization term, which also enters the momentum balance as a third-order Korteweg-like term. Moreover, using the variational structure, we are able to introduce gravity consistently into both the momentum equation and the diffusion equation, *e.g.*, leading to correct equilibrium states via the barometric formula. However, while $\boldsymbol{\eta}$ is the correct chemical potential for this (isothermal) system, note that π is not the (full) thermodynamic pressure but only the Biot-type pore pressure contribution.

We are going to solve this problem in two spatial dimensions in a rectangular domain $\Omega = (0, L) \times (0, H)$ with components $x = (x_1, x_2) \in \Omega$ and with initial data

$$\boldsymbol{u}_0(x) = 0\,, \qquad c_0(x) = \bar{c}_0 + \bar{c}_1\exp(-\tfrac{1}{r^2}|x - x_0|^2)\,. \tag{23}$$

We impose sliding wall boundary conditions $\boldsymbol{u}(t)\cdot\boldsymbol{\nu} = 0$ for $x_1 \in \{0, L\}$ and no-slip boundary conditions for $x_2 \in \{0, H\}$ on the boundary. For the fluid content c we employ homogeneous natural boundary conditions. The nondimensional domain size is $L = 1$ and $H = 2$ and in the initial data we use $r = 1/5$. We use $\bar{c}_0 = 10^{-2}$ and $\bar{c}_1 = 5\cdot 10^{-2}$ and viscosity $\nu = 10^{-3}$. For gravity we use $g = (0, g_0)$, where g_0 and the remaining parameters are given in Table 1. Both simulations use 300 time steps to reach the final time T.

Table 1: Comparison of selected parameters for flowing and diffusive regimes.

Parameter	flowing regime	diffusive regime
g_0	-0.1	-0.01
D_0	0.1	1000
ε	10^{-3}	10^{-5}
μ	10^{-9}	10^{-3}
T	10.0	4.0

We present in Figure 2 and Figure 3 two examples of different types of porosity waves, where the main difference is that the parameters give rise to a transport of fluid content primarily by convection in the former, *i.e.*, the *flowing regime*, and primarily by diffusion in the latter, *i.e.*, the *diffusive regime*. This is achieved by the different sets of parameters shown in Table 1, where in the flowing regime the shear modulus, but also the diffusion constant, are both very small, whereas in the diffusive regime we suppress flow by a larger shear modulus and enhance diffusion by a larger diffusion constant. Without going into the details of the solution, this difference is most prominently observed in Figure 4, where in the flowing regime the dissipation from diffusion, encoded in $k(\eta, \eta)$, is practically negligible, whereas in the diffusive regime the Kelvin–Voigt viscous dissipation, encoded in $g(\partial_t\boldsymbol{q}, \partial_t\boldsymbol{q})$, is similarly negligible. If one looks at the individual contributions (elastic, Biot, gravity, regularisation), one observes that primarily gravity $H_{\mathrm{grav}}(c)$ changes, while the other contributions leave the porosity wave almost in local equilibrium, *i.e.*, their contributions to the energy are very small.

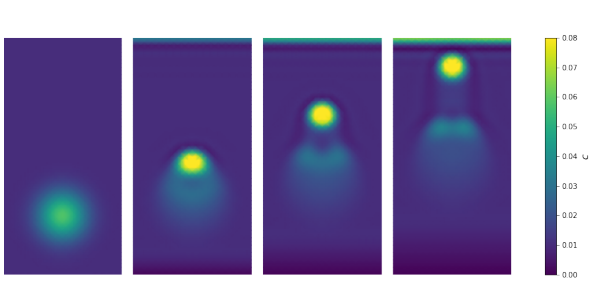

(a) Concentration c for time advancing from left to right.

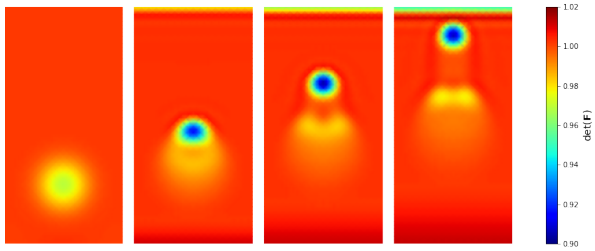

(b) Determinant $J = \det \boldsymbol{F}$ for time advancing from left to right.

Figure 3: Porosity wave moving fluid upwards and displacing the (elastic) material in the **diffusive regime** at times $t = 0, 4/3, 8/3, 4$.

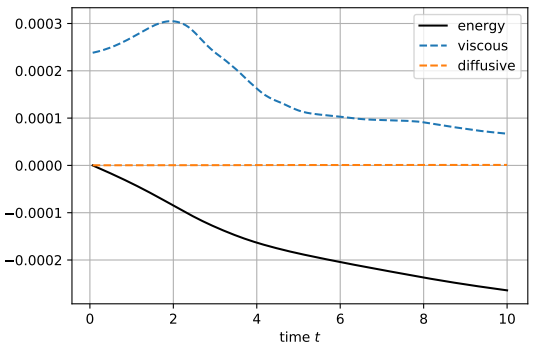

(a) Flowing regime

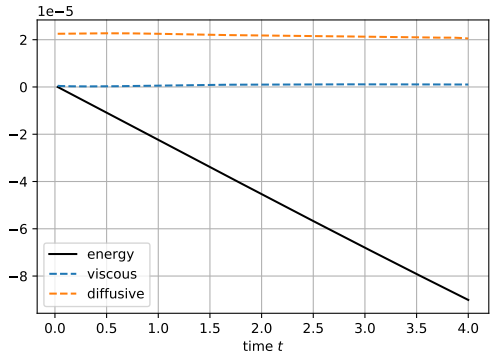

(b) Diffusive regime

Figure 4: Decreasing system energy $\mathscr{H}(\boldsymbol{q}(t))$ (black line) and viscous dissipation $g(\partial_t \boldsymbol{q}, \partial_t \boldsymbol{q})$ (blue dashed line) and diffusive energy loss $k(\eta, \eta)$ (orange dashed line) as a function of time t.

The interpretation of these shapes is somewhat limited by the fact that several simplifications are applied here, *i.e.*, the geometry is two-dimensional, and compaction of the solid phase due to gravity is neglected. This is both because a term $J^{-1}\varrho_0 x \cdot g$ is missing in the energy, and because the overall domain is fixed. The latter could be circumvented by introducing an additional indicator function for a fictitious air phase, as in [18]. The main difference is that in the flowing regime, the porosity wave tends to grow in extent and leaves a more pronounced wake behind, whereas in the diffusing regime, with degenerate diffusion $D(c) = c^2 D$, the porosity wave tends to develop a more compact support.

Summary

We developed an Eulerian model for poroelasticity that is energy-based and supports large deformations using a reference map approach. The discretisation is structure-preserving and therefore allows for a straightforward discretisation in space using finite elements and in time using an incremental (finite-difference-type) scheme. We employ this model to present different types of porosity waves, in which the fluid content is transported either by flow or by diffusion.

References

[1] Yury Alkhimenkov, Lyudmila Khakimova, and Yury Podladchikov. Shear bands triggered by solitary porosity waves in deforming fluid-saturated porous media. *Geophysical Research Letters*, 51(15):e2024GL108789, 2024.

[2] Nicolás Barnafi, Paolo Zunino, Luca Dedè, and Alfio Quarteroni. Mathematical analysis and numerical approximation of a general linearized poro-hyperelastic model. *Computers & Mathematics with Applications*, 91:202–228, 2021.

[3] Peter Betsch and Mark Schiebl. Energy-momentum-entropy consistent numerical methods for large-strain thermoelasticity relying on the GENERIC formalism. *International Journal for Numerical Methods in Engineering*, 119(12):1216–1244, 2019.

[4] Maurice A. Biot. General theory of three-dimensional consolidation. *Journal of Applied Physics*, 12(2):155–164, 1941.

[5] Maurice A. Biot. Theory of propagation of elastic waves in a fluid-saturated porous solid. i. low-frequency range; ii. higher frequency range. *The Journal of the Acoustical Society of America*, 28:168–191, 1956.

[6] Maurice A. Biot. Mechanics of deformation and acoustic propagation in porous media. *Journal of Applied Physics*, 33:1482–1498, 1962.

[7] Piero Chiarelli, Bruna Vinci, Antonio Lanatà, Clara Lagomarsini, and Simone Chiarelli. Poroelastic longitudinal wave equation for soft living tissues. *Journal of Biorheology*, 28(1):29–37, 2014.

[8] Herbert Egger and Mania Sabouri. On the structure preserving high-order approximation of quasistatic poroelasticity. *Mathematics and Computers in Simulation*, 189:237–252, 2021.

[9] Miroslav Grmela and Hans Christian Öttinger. Dynamics and thermodynamics of complex fluids. I. Development of a general formalism. *Physical Review E*, 56(6):6620, 1997.

[10] Ansgar Jüngel, Ulisse Stefanelli, and Lara Trussardi. A minimizing-movements approach to GENERIC systems. *arXiv preprint arXiv:2005.14437*, 2020.

[11] Ken Kamrin, Chris H Rycroft, and Jean-Christophe Nave. Reference map technique for finite-strain elasticity and fluid–solid interaction. *Journal of the Mechanics and Physics of Solids*, 60(11):1952–1969, 2012.

[12] Chun Liu and Noel J Walkington. An Eulerian description of fluids containing visco-elastic particles. *Archive for Rational Mechanics and Analysis*, 159:229–252, 2001.

[13] Dan McKenzie. The generation and compaction of partially molten rock. *Journal of Petrology*, 25(3):713–765, 1984.

[14] Alexander Mielke. Formulation of thermoelastic dissipative material behavior using GENERIC. *Continuum Mechanics and Thermodynamics*, 23(3):233–256, 2011.

[15] Philip J Morrison. Hamiltonian description of the ideal fluid. *Reviews of Modern Physics*, 70(2):467, 1998.

[16] Hans Christian Öttinger and Miroslav Grmela. Dynamics and thermodynamics of complex fluids. II. Illustrations of a general formalism. *Physical Review E*, 56(6):6633, 1997.

[17] Felix Otto. The geometry of dissipative evolution equations: the porous medium equation. *Communications in Partial Differential Equations*, 26(1-2):101–174, 2001.

[18] Dirk Peschka, Marita Thomas, and Andrea Zafferi. Reference map approach to eulerian thermomechanics using generic. *WIAS preprint*, (3178), 2025. Accepted in *Advances in Continuum Physics*. DOI 10.20347/WIAS.PREPRINT.3178.

[19] Dirk Peschka, Andrea Zafferi, Luca Heltai, and Marita Thomas. Variational approach to fluid-structure interaction via generic. *Journal of Non-Equilibrium Thermodynamics*, 47(2):217–226, 2022.

[20] Kaare Brandt Petersen, Michael Syskind Pedersen, et al. The matrix cookbook. *Technical University of Denmark*, 7(15):510, 2008.

[21] Tomas Roubicek and Ulisse Stefanelli. Thermodynamics of elastoplastic porous rocks at large strains towards earthquake modeling. *SIAM Journal on Applied Mathematics*, 78(5):2597–2625, 2018.

[22] Tomáš Roubíček and Ulisse Stefanelli. Viscoelastodynamics of swelling porous solids at large strains by an Eulerian approach. *SIAM Journal on Mathematical Analysis*, 55(4):2677–2703, 2023.

[23] Leonie Schmeller and Dirk Peschka. Gradient flows for coupling order parameters and mechanics. *SIAM Journal on Applied Mathematics*, 83(1):225–253, 2023.

[24] Rob M Skarbek and Alan W Rempel. Dehydration-induced porosity waves and episodic tremor and slip. *Geochemistry, Geophysics, Geosystems*, 17(2):442–469, 2016.

[25] Meng Tian and Jay J Ague. The impact of porosity waves on crustal reaction progress and co2 mass transfer. *Earth and Planetary Science Letters*, 390:80–92, 2014.

[26] Willem JM van Oosterhout and Matthias Liero. Finite-strain poro-visco-elasticity with degenerate mobility. *ZAMM-Journal of Applied Mathematics and Mechanics/Zeitschrift für Angewandte Mathematik und Mechanik*, 104(5):e202300486, 2024.

[27] Chaozhen Wei and Min Wu. An eulerian nonlinear elastic model for compressible and fluidic tissue with radially symmetric growth. *SIAM Journal on Applied Mathematics*, 83(1):254–275, 2023.

[28] Andrea Zafferi, Dirk Peschka, and Marita Thomas. GENERIC framework for reactive fluid flows. *ZAMM-Journal of Applied Mathematics and Mechanics/Zeitschrift für Angewandte Mathematik und Mechanik*, 103(7):e202100254, 2022.